J. Membrane Biol. 11, 21 – 46 (1973)

Calcium-Calcium and Calcium-Strontium Exchange across the Membrane of Human Red Cell Ghosts

H. Porzig

Pharmakologisches Institut, Universität Bern, Switzerland

Received 2 June 1972

Summary. Stationary and nonstationary state ^{45}Ca fluxes as well as Sr–Ca exchange movements were studied in energy-depleted human erythrocyte ghosts at different intra- and extracellular Ca concentrations. Influx and efflux followed the kinetics of a closed two-compartment system. The influx and efflux rate constants (k_{in} and k_{out}, respectively, fractions of total extra- or intracellular ^{45}Ca that move in one direction per unit time) were similar in magnitude. They decreased with increasing Ca concentration on the cis-side and increased with increasing Ca concentration on the trans-side of the membrane. Hence, the fluxes in both directions were characterized by saturation kinetics and appeared to be partially caused by an exchange diffusion mechanism. In the presence of a moderate inward (up to 8 mM) or outward (up to 2 mM) Ca concentration gradient, k_{in} and k_{out} did not vary in the course of an experiment and did not differ significantly from rates which were measured under stationary state conditions. Extracellular Sr induced an outward transport of intracellular Ca against the concentration gradient (countertransport). The resulting inward Ca concentration gradient (maximal inside-to-outside concentration ratio as 1 to 3) persisted since extra- and intracellular Sr did not equilibrate. Analogous results were obtained studying ^{45}Ca–^{40}Ca countertransport. In net flow experiments Ca–Sr exchange proved to occur on a one-for-one basis. Ca–Sr exchange was additive to the noncoupled Ca and Sr net downhill movements. The experimental results suggest that a specific ATP-independent Ca transfer system exists in the erythrocyte membrane which acts symmetrically on the two sides of the membrane and is restricted to a tightly coupled one-for-one exchange diffusion.

In animal tissues, two different types of membrane transport systems enabling the cell to extrude Ca against the existing concentration gradient and to maintain a low intracellular Ca level have been characterized. In mammalian cardiac muscle, squid axon, and rabbit vagus nerve, calcium outflow depends on extracellular Na concentration. It was suggested that this reflects a coupling of Ca outflow to Na inflow by an exchange diffusion mechanism (Reuter & Seitz, 1968; Blaustein & Hodgkin, 1969; Kalix, 1971). Direct evidence for a coupling of Ca and Na fluxes in the opposite direction

(i.e., Ca inflow to Na outflow) was obtained by Baker, Blaustein, Hodgkin and Steinhardt (1969) in squid axon. In red cells, liver cells and tissue-cultured L-cells, net Ca outward transport was reported to depend directly on *high* energy compounds and not to be coupled to the movement of other ions (Schatzmann & Vincenzi, 1969; van Rossum, 1970; Lamb & Lindsay, 1971). However, in a previous study concerned with passive ^{45}Ca efflux from human erythrocyte ghosts, a saturable ATP-independent Ca–Ca exchange mechanism could be demonstrated (Porzig, 1970). This observation led to the postulation of an additional specific Ca transport mechanism mediating passive Ca movements across the red cell membrane. When the ghosts were energy depleted, downhill net movements of Ca under the influence of similar inward or outward concentration gradients proved to be asymmetric. Net inflow ceased well before equilibrium between intra- and extracellular concentrations was established. Net outflow was larger than inflow and increased throughout the experimental period of time. To account for this asymmetric behavior, it was proposed that calcium might bind to specific permeability controlling sites in the cell membrane (Porzig, 1972).

In the present study, the possibility that an asymmetry in the Ca transfer system could offer an alternative explanation for nonequilibration in downhill Ca net movements was tested. Moreover, to further characterize the ATP-independent Ca transfer system, Ca movements were studied in the presence of Sr which competes with Ca for transport sites. The experimental results suggest two different pathways for passive Ca transmembrane movements in red cell ghosts: (1) a specific saturable system mediating a one-for-one exchange diffusion, and (2) a nonspecific, nonsaturating "leak" pathway.

Materials and Methods

One-day-old human red blood cells sedimented from ACD-stabilized blood were obtained from the Swiss Red Cross Blood Transfusion Service in Bern and were stored in the laboratory refrigerator at 4 °C for 1 to 6 days prior to use. The methods used to starve the cells and to prepare Ca-free and Ca-loaded erythrocyte ghosts by reversible osmotic hemolysis were described previously (Porzig, 1970, 1972). The concentration ratio of Ca between ghost cells and medium ($[Ca]_i/[Ca]_o$) at the end of the equilibration period following reversal of hemolysis depended on the Ca concentration in the hemolyzing fluid ($[Ca]_{hem}$). The $[Ca]_i/[Ca]_o$ was close to 1 when $[Ca]_{hem}$ was 0.1 to 0.25 mM and dropped to about 0.6 when Ca_{hem} was 4 mM. In control experiments, $[Ca]_i/[Ca]_o$ remained nearly unchanged even when the equilibration period was extended from 60 to 240 min. Therefore, $[Ca]_i/[Ca]_o$ at the end of the equilibration period was considered to represent the stationary state calcium distribution.

Tracer Flux Experiments

To study unidirectional tracer fluxes without interference from net movements of nonradioactive Ca, ^{45}Ca (30 to 90 μC/100 ml) was added to the suspension at the end of the equilibration period. The uptake of tracer into the ghosts was then followed during the subsequent 180 min. In experiments measuring nonstationary state Ca flux, the reconstituted ghosts were washed 3 times in ice cold Ca-free standard medium (145 mM KCl, 20 mM Tris-Cl, pH 7.4) after the equilibration period. They were then transferred to the prewarmed (37 °C) experimental medium, and incubated for 180 min. Unless otherwise stated, the experimental medium was the same as the standard medium but contained variable amounts of Ca. In influx experiments, tracer amounts of ^{45}Ca were added to the final incubation medium. In efflux studies, ^{45}Ca was a constituent of the hemolyzing fluid. In experiments designed to study ^{45}Ca–^{40}Ca or ^{45}Ca–Sr counterflow, 30 to 90 μC of tracer were added to the hemolyzing medium to establish identical specific activities on both sides of the membrane.

The cellular radioactivity in the stationary state was measured at the end of the equilibration period and immediately preceding the addition of cold Ca or Sr to the external medium. The change in cellular radioactivity was then followed for 180 or 240 min.

Preparation of Samples

Samples of 0.2 ml were drawn from the incubation suspensions at suitable intervals by means of a fixed volume micropipette (Eppendorf) and transferred into 9.8 ml of ice cold isotonic choline solution buffered to pH 7.4. The extracellular radioactivity was thus diluted by a factor of 50. A sample of 5 ml of the diluted ghost suspension containing 2.5 μliters of cells was filtered according to the method of Wilbrandt and Becker (*unpublished*) using membrane filters with a mean pore size of 3 μ (Sartorius) and applying a maximal suction of 10 cm H_2O. A single filtration took about 5 sec. To test if a significant amount of cells was destroyed during the filtration procedure, the time course of ^{45}Ca efflux from tracer-loaded ghosts was followed for 3 hr. Cells and medium were then separated either by filtration or by centrifugation. No differences in the results could be detected. The filters with the adhering cells were dried overnight and placed in counting vials. A sample of 10 ml of a toluene-BBOT scintillation fluid (2.5-*bis*-5-tert: butylbenzoxazolyl-2-tiophen (BBOT, Ciba) 2 g/liter of toluene) was added and the samples counted in a Nuclear Chicago Mark II liquid scintillation counter. Blanks without cells were prepared to account for extracellular radioactivity trapped in the filters. No radioactivity was lost from the filter into the fluid. To measure the total radioactivity in the cell suspension and the supernatant, 1-ml samples were wet-ashed, dissolved in 0.1 M HCl, and counted in 10 ml of Bray's scintillation liquid (*cf.* Porzig, 1970). Control experiments showed that the counting efficiency was higher in Bray-dissolved samples than in the filter-BBOT/toluene-system. Therefore, a correction factor was experimentally determined and applied to assure the comparability of sample counts obtained with the two methods.

Evaluation of Flux Data

As shown in a preceding study on ^{45}Ca efflux (Porzig, 1970), the experimental ghost suspension with respect to ^{45}Ca fluxes can be treated in reasonable approximation as a closed two-compartment system. The general equation describing the rate of change in internal concentration with time in such a system is

$$\frac{d^*C_i}{dt} = k_{in}{}^*C_o - k_{out}{}^*C_i \tag{1}$$

(where $^*C_i$ and $^*C_o$ are the inside and outside tracer concentrations, respectively, k_{in} and k_{out} are the rate constants for inward and outward movement of tracer). and k_{out} give the fraction of total intra- and extracellular ^{45}Ca that moves in one direct per unit time. Both rate constants can be evaluated in the same experiment provided external volume is large compared to that of the cells. In this case, the change in * with time will be negligibly small and the product $(k_{in} \cdot {}^*C_o)$ can be treated as a consta Hence, the integration of Eq. (1) yields an exponential equation which is characteriz only by k_{out} and $^*C_i$

$$^*C_i^t = {}^*C_i^\infty - {}^*C_i^\infty \exp(-t k_{out}) \quad (2)$$

where $^*C_i^t$ is the intracellular tracer concentration at time t and $^*C_i^\infty$ is the stationa state intracellular tracer concentration. A semilog plot of the differences at any giv time between $^*C_i^t$ and $^*C_i^\infty$ will result in a straight line with the slope equal to k_o Assuming that the rate of change of $^*C_i$ in the first minutes of the experiments depen only on k_{in}, this constant could be calculated in the same experiments from the initi velocity of tracer uptake. If the system were in a stationary state with respect to t bulk concentration of Ca, the rate constants for tracer movements could also be evaluate according to a method suggested by Ekman, Manninen and Salminen (1969) and Ma ninen (1970). These authors derived an equation for k_{in}

$$k_{in} = \frac{B/t}{\frac{V_i}{V_o} + \frac{1}{^*r^\infty}}, \qquad B = \ln \frac{1 + {}^*r\, V_i/V_o}{r - {}^*r/{}^*r^\infty} \quad (3)$$

which is based on the relationships expressed in Eqs. (1), (4) and (5). The total amou of tracer in the system is constant, thus

$$\frac{V_o\, d\,{}^*C_o}{dt} + \frac{V_i\, d\,{}^*C_i}{dt} = 0. \quad (4)$$

In the stationary state

$$\frac{^*C_i^\infty}{^*C_o^\infty} = {}^*r^\infty = \frac{k_{in}}{k_{out}} \quad \text{holds.} \quad (5)$$

V_o is the volume of the medium and V_i is the volume of the cells. $^*r$ is defined a $^*C_i/{}^*C_o$ and r is C_i/C_o, C_i and C_o being the inside and outside concentrations of nor radioactive (traced) substance.

The plot of B *vs.* t yields a straight line since

$$B = t k_{in} \left[\frac{V_i}{V_o} + \frac{^*C_o^\infty}{^*C_i^\infty} \right] \quad (6)$$

with the slope given by

$$k_{in} \left[\frac{V_i}{V_o} + \frac{^*C_o^\infty}{^*C_i^\infty} \right].$$

By using Eqs. (6) and (5), k_{in} and k_{out} can then be calculated.

Determination of Ca, Sr and Mg Net Movements

The method used for the net flow experiments and the determination of Ca an Mg by atomic absorption photometry were described earlier (Porzig, 1972). In the sam samples, Sr was also measured by atomic absorption. Sr stock solutions were prepare

from $SrCl_2 \cdot 6\,H_2O$. The SrCl, concentration in the main stock solution was measured by chloride titration using potassium bichromate as indicator.

The hematocrit of the experimental ghost suspensions in ^{45}Ca flux measurements and in net flow studies was measured using van Allen hematocrit tubes (Porzig, 1971).

Concentrations are given in mM/liter solution or mM/liter ghosts, respectively. The pH of the experimental solutions was adjusted with Tris-Cl to 7.4 at 20 to 22 °C (corresponding to 7.2 at 37 °C and 7.7 at 1 °C.)

Results

Unidirectional ^{45}Ca Fluxes

The first set of experiments was designed to study stationary state ^{45}Ca influx and efflux rates. This would establish whether the ATP-independent Ca-transfer system acted symmetrically on the two sides of the membrane.

Fig. 1 (*a*) illustrates the time course of stationary state tracer uptake into human red cell ghosts at different calcium concentrations. The stationary state under these conditions was characterized by the absence of any measurable net Ca movements. However, this did not necessarily imply that $[Ca]_i$ (total cellular Ca) and $[Ca]_o$ (extracellular Ca) were equal. The actual concentrations on the two sides of the membrane are shown by the figure on the right side of curves I–III in Fig. 1(*a*). As can be judged from the initial velocities, the rate of tracer uptake (k_{in}) decreased with increasing Ca concentration. The calculated values from this experiment were 0.0269, 0.0110 and 0.0057 min^{-1}, respectively. It should be noted that ^{45}Ca uptake between zero time of the experiment (addition of tracer) and withdrawel of the first sample ($\sim$2 min) was disregarded and not used for the evaluation of the rate constants. Therefore, rapid ^{45}Ca–^{40}Ca exchange reactions at the cell surface should not interfere with these measurements.

The efflux rates (k_{out}) can be calculated from the same experimental data only if the stationary state values of $^*C_i^\infty$ are known.

Fig. 1(*a*) shows that only in the presence of the low Ca concentration was the stationary state for tracer uptake reached within 180 min (curve I). When Ca concentrations were higher than 0.125 mM (curves II and III), it was necessary to extrapolate for $^*C_i^\infty$. By trial and error a value was chosen which gave the best linear fit in a semilog plot of $^*C_i^\infty - {}^*C_i^t$ where $^*C_i^t$ is the intracellular radioactivity at any particular time. This procedure seemed to be justified by the previous finding that Ca efflux from human red cell ghosts follows the kinetics of a simple two-compartment system (Porzig, 1970). The results of applying this approach to the three uptake curves in Fig. 1(*a*) are shown in Fig. 1(*b*). Straight lines are a reasonable

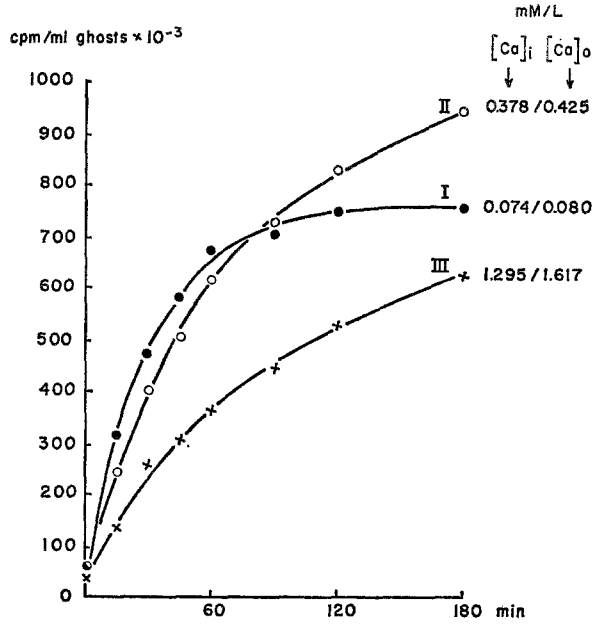

Fig. 1 a

Fig. 1. (*a*) Time course of unidirectional ^{45}Ca influx in red cell ghosts. Tracer uptake in cpm per ml ghosts (ordinate) is plotted against time (abscissa) in min. Red cells were hemolyzed in a solution containing 4 mM $MgCl_2$, 8 mM Tris–Cl and three different Ca concentrations, 0.1 mM (curve I, •—— •), 0.5 mM (curve II, ○——○) and 2 mM (curve III, ×——×). Reversal of hemolysis with KCl. After 60 min of equilibration, the experiment was started by adding 1 μC/ml tracer Ca. The numbers on the right of each curve give $[Ca]_i$ and $[Ca]_o$ in mM/liter. These concentrations remained unchanged during the experiment. One of 6 similar experiments. Hematocrit: 2.85 to 3.0%. (*b*) Semilog plot of the differences between intracellular tracer concentration extrapolated for infinite time ($^*C_i^\infty$) and tracer concentration at each particular time t($^*C_i^t$), for curves I–III in Fig. 1 (*a*). *Ordinate*: log ($^*C_i^\infty - {}^*C_i^t$). *Abscissa*: time in min, linear scale. The numerical values for $^*C_i^\infty$ were extrapolated by trial and error to give the best linear fit. The numerical values for k_{out} (k min^{-1}) calculated from the slopes of the straight lines are indicated on the right

fit for the experimental points. The efflux rates as calculated from the slopes of these lines are indicated on the right in Fig. 1 (*b*). If $[Ca]_i$ was raised from 0.074 to 1.295 mM/liter of ghosts, k_{out} decreased from 0.0303 to 0.0104 min^{-1}.

The method used to evaluate the two rate constants as demonstrated in Fig. 1 (*a*) and (*b*) (method I) could also be used in flux experiments where the system was not in a stationary state with respect to the bulk concentrations (*see below*). The stationary state approach, however, allowed checking the results of method I by comparing them with the results obtained

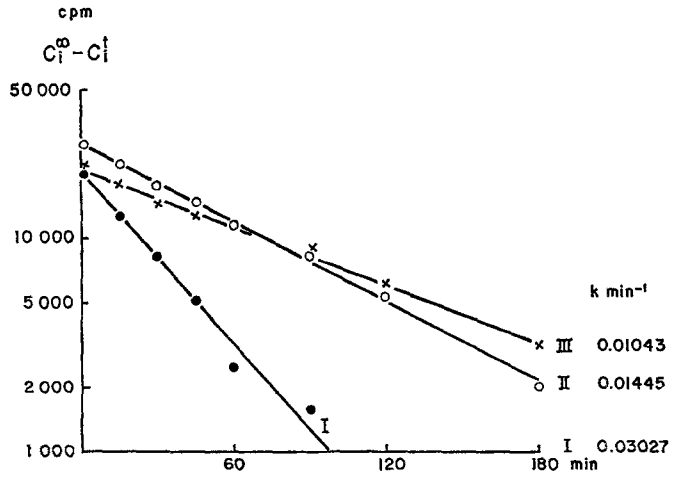

Fig. 1 b

when Eqs. (3), (5) and (6) were applied to the same data (using the same numerical values for $^*C_i^\infty$). The fact that the two methods of extracting rate constants gave the same values, was considered a valuable test, particularly for the validity of estimating k_{in} by measuring initial velocities.

The data for all stationary state experiments are summarized in the plot of k_{in} vs. $[Ca]_o$ and k_{out} vs. $[Ca]_i$ shown in Fig. 2. The figure shows a decrease of k_{out} with increasing $[Ca]_i$, (*cf.* Porzig, 1970), which indicates saturation kinetics for efflux. The influx rates in the same experiments, although always smaller than the corresponding efflux rates, were similarly related to $[Ca]_o$ and decreased from 0.0125 to 0.003 min^{-1} when $[Ca]_o$ was raised from 0.08 to 3.29 mM. Hence, saturation kinetics did apply for influx as well. The consistent difference in the numerical values for k_{in} and k_{out} at any particular Ca concentration, however, was somewhat confusing since it suggested a striking asymmetry in the unidirectional Ca fluxes. A calculation of the unidirectional fluxes based on the data of Fig. 2, at the same Ca concentration yielded values for efflux considerably larger than for influx. A flux ratio different from unity under these conditions, however, was incompatible with the existence of a stationary state which, by definition, required equal fluxes in both directions to prevent a net ionic movement. The examination of the specific activities of cellular Ca extrapolated to infinite time revealed that only part of the total cellular Ca (as measured by the atomic absorption method) took part in Ca exchange. Hence, the outward rates in Fig. 2 correspond to lower "effective" Ca concentrations than indicated. The size of the "nonexchangeable" fraction (Ca_{inex}) varied between 13 and 46% of total intracellular Ca. The dashed curve in Fig. 2

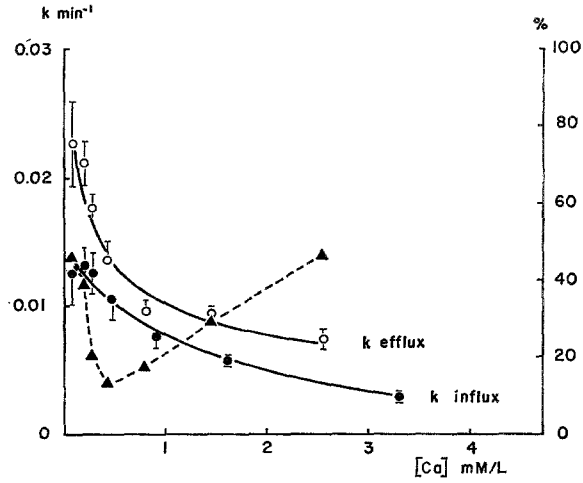

Fig. 2. Dependence of stationary state rate constants for ^{45}Ca influx and efflux (left ordinate, min^{-1}) on the Ca concentration on the cis-side of the membrane (abscissa, mM/liter). Same ghost preparation as in Fig. 1(*a*). k_{in} is plotted *vs.* $[Ca]_o$ (●——●), k_{out} *vs.* $[Ca]_i$ (○——○). The numerical values for the two rate constants were calculated from the data of 6 similar experiments according to Eqs. (3), (5) and (6). The dashed line (▲-- ▲) shows the nonexchangeable fraction of cellular Ca as per cent of $[Ca]_i$ (right ordinate). The points are mean values of 3 to 5 measurements. Vertical bars: ± SE Hematocrit: 2.5 to 4.2%

illustrates the relationship between Ca_{inex} and $[Ca]_i$. It depicts the nonexchangeable Ca as per cent of total cellular Ca. This fraction is not completely unexchangeable but had an exchange rate too slow to be detected in these experiments.

If k_{out} in Fig. 2 is replotted as a function of exchangeable cellular Ca instead of total $[Ca]_i$, the curves for k_{in} and k_{out} in Fig. 2 do not perfectly coincide, but the differences in the numerical values of the corresponding unidirectional fluxes are statistically no longer significant. This can be inferred from Fig. 3. In this figure, the unidirectional Ca efflux in μM/min per ml ghosts is plotted as a function of the cellular exchangeable Ca concentration and is compared to unidirectional influx as a function of $[Ca]_o$. The efflux curve does not extend to a Ca concentration range beyond 1.2 mM because of the decrease in the fraction of exchangeable Ca with increasing $[Ca]_i$. The fluxes clearly show saturation kinetics similar to those previously derived from the behavior of the rate constants.

To test whether Michaelis-Menten kinetics might be applicable to the stationary state rate constants of Fig. 2. $1/k_{in}$ was plotted against $[Ca]_o$ and $1/k_{out}$ was plotted against *exchangeable* $[Ca]_i$ (*cf.* Riggs, 1963) (Fig. 4).

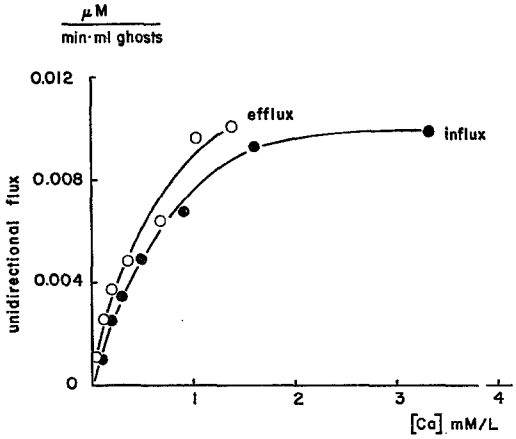

Fig. 3. Relation between unidirectional fluxes (in μM/min per ml ghosts, ordinate) and cis-side Ca concentration (abscissa, mM/liter). The influx (○——○) was calculated by multiplying k_{in} with $[Ca]_o$. To calculate the efflux (●——●), k_{out} was multiplied with the exchangeable fraction of total cellular Ca. Data taken from Fig. 2

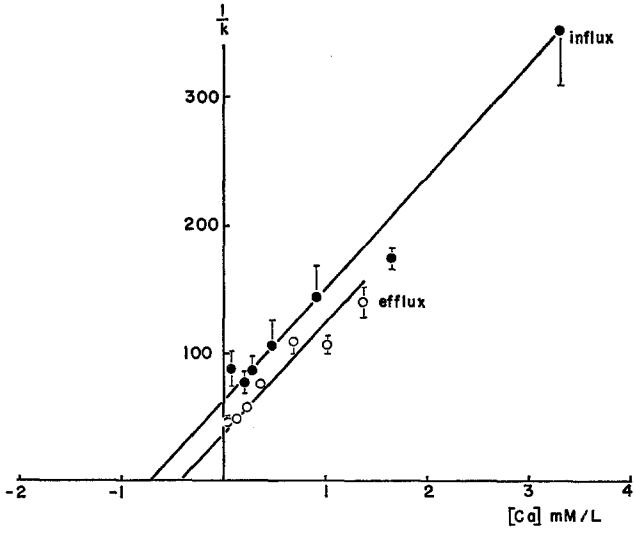

Fig. 4. Plot of $1/k_{in}$ *vs.* $[Ca]_o$ (●——●) and of $1/k_{out}$ *vs.* the exchangeable fraction of total cellular Ca (○——○). Same data as in Fig. 2. Vertical bars: ± SE; no bar: SE smaller than symbol. The *Km* values (intercept with the abscissa) are 0.75 mM for influx and 0.4 for efflux. v_{max} (reciprocals of the slopes of the straight lines) was 0.0113 mM/min

Straight lines can be fitted to the experimental points. Note that in this plot the slopes are equal to $1/v_{max}$ and *Km* is equal to the intercepts on the abscissa. Ca influx and efflux have a similar v_{max} but seem to differ in *Km*

(0.75 mM for influx and 0.32 mM for efflux). However, the "effective" intracellular Ca concentration determining the flux rate may be overestimated if it is assumed to be equal to the exchangeable fraction of cellular Ca (*see* Discussion, p. 42). It is therefore rather doubtful whether this difference in the *Km* values is of significance.

Dependence of k_{in} and k_{out} on $[Ca]_i$ and $[Ca]_o$ in Nonstationary State Experiments

To avoid net Ca movements in stationary state experiments, the concentrations of nonradioactive Ca had to be changed simultaneously on the two sides of the membrane. Therefore, these studies could not provide any information about the influence of Ca concentration on the trans-side of the membrane on tracer kinetics. In two series of experiments, the dependence of the rate constants on $[Ca]_i$ at constant $[Ca]_o$ and on $[Ca]_o$ at constant $[Ca]_i$ was examined. k_{in} and k_{out} are plotted as functions of $[Ca]_i$ in Fig. 5 and in Fig. 6, the two rate constants are plotted as functions of $[Ca]_o$.

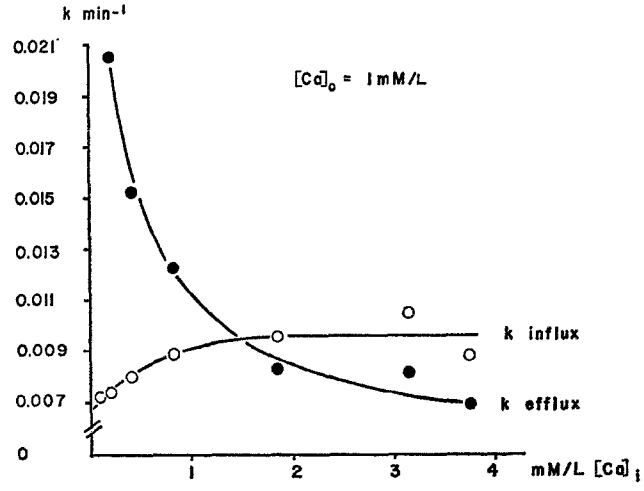

Fig. 5. Dependence of ^{45}Ca influx and efflux rate constants (ordinate, min^{-1}) on total cellular Ca concentration (abscissa, mM/liter). Starved red cells were hemolyzed in solutions containing 4 mM $MgCl_2$, 8 mM Tris–Cl and different Ca concentrations (0.25, 0.5, 1, 2, 4, 5 mM). Reversal of hemolysis with KCl. After equilibration for 70 min at 37 °C, the ghosts were washed twice in Ca-free solution (145 mM KCl, 20 mM Tris–Cl, pH 7.4) and once in a Ca-containing solution (145 mM KCl, 20 mM Tris–Cl, 1 mM $CaCl_2$, pH 7.4). The cells were then incubated at 37 °C in this latter solution containing in addition ^{45}Ca (1 μC/ml). k_{out} (•——•) was evaluated as shown in Fig. 1 (*b*). k_{in} (○ — — ○) was calculated from the initial velocities of tracer uptake. One of 3 similar experiments. Hematoctit: 2.4 to 3.3%. Comparable results were obtained in 6 other experiments where the main cation in the external medium was Na instead of K

Except for the tested Ca concentrations, the conditions of the two experiments from which the data were taken were identical. It is evident from Figs. 5 and 6 that the flux rates under both conditions showed very similar characteristics. The influx as well as the efflux transport rates were stimulated by an increase of the Ca concentration on the trans-side of the membrane. When total cellular Ca was raised from 0.1 to 1.8 mM, k_{in} increased from 0.0072 to 0.0095 min^{-1} (Fig. 5) whereas a change in $[Ca]_o$ from 0.1 to 1.0 mM induced a shift in k_{out} from 0.0085 to 0.0125 min^{-1} (Fig. 6).

Trans-activation was also a saturable process. The trans-side Ca concentration necessary to reach maximal activation seemed higher for influx than for efflux. Yet, this effect, like the asymmetry observed with unidirectional fluxes, was at least partially caused by the fact that total cellular Ca (abscissa of Fig. 5) was not entirely exchangeable and that the exchangeable fraction did not depend on $[Ca]_i$ in a linear fashion. In addition, it should be pointed out that extrapolation to zero of the curve for k_{in} in Fig. 5 does not give the rate of net Ca inward movement into Ca-free ghosts. At cellular Ca concentrations below 0.1 mM the Ca binding capacity of the

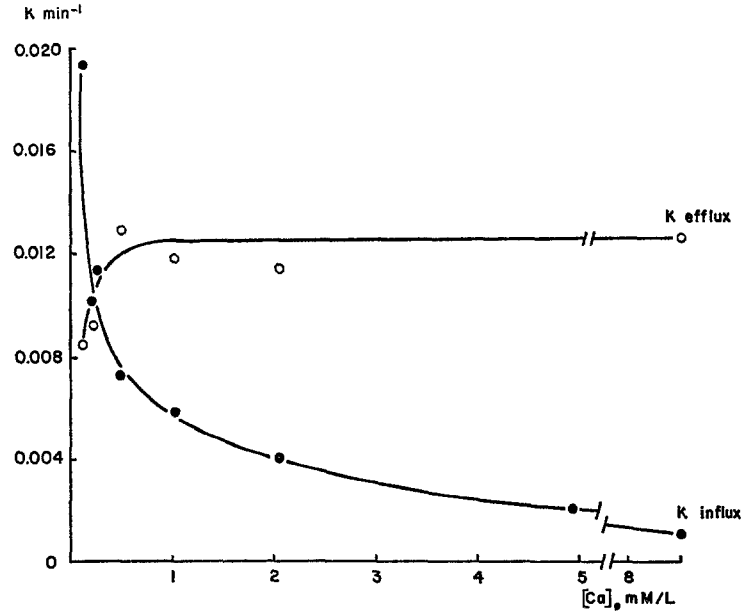

Fig. 6. Dependence of ^{45}Ca influx and efflux rate constants (ordinate, min^{-1}) on $[Ca]_o$ (abscissa, mM/liter). Preparation of ghosts as in Fig. 5. The hemolyzing solution contained 1 mM $CaCl_2$. After equilibration, the ghosts were washed three times in Ca-free solution (145 mM KCl, 20 mM Tris–Cl, pH 7.4) and then incubated in solutions containing 145 mM KCl, 20 mM Tris–Cl, Ca concentrations ranging from 0.1 to 8 mM and 1.3 μC/ml ^{45}Ca (pH 7.4). k_{in} (●——●) and k_{out} (○ – – ○) were evaluated as in Fig. 5. One of 7 similar experiments. Hematocrit: 3.5 to 4.1 %

ghost membrane increases to such an extent that the rate of cellular Ca uptake will be mainly determined by the rate of Ca binding to membrane sites (*cf.* Porzig, 1972). Control experiments in connection with the present work showed indeed, that the initial rate of Ca uptake was lower in ghosts containing 0.1 mM Ca than in virtually Ca-free ghosts. The interference between Ca binding and Ca exchange rates at low $[Ca]_i$ and the resulting overestimation of k_{in} tends to decrease the apparent trans-activation component of k_{in}.

Influx and efflux had in common the decrease in rate with increasing Ca concentration on the cis-side of the membrane. This was expected from the stationary state experiments (Fig. 2). The constant Ca concentration on the trans-side in both cases was about 1 mM and hence always in the range of maximal trans-activation. The numerical values for k_{out} in Fig. 5 and k_{in} in Fig. 6 (and those of all comparable experiments) were found to be in good agreement with the corresponding values in Fig. 2. The similarity of ^{45}Ca flux kinetics under stationary and nonstationary state conditions suggested that net intracellular Ca concentration changes were small even in the presence of moderate inward or outward driving forces. Therefore, the Ca fluxes measured in nonstationary state experiments were likely to represent largely Ca–Ca exchange.

A plot of $1/k_{in}$ *vs.* $[Ca]_o$ as in Fig. 3 yielded a straight line with nearly the same Km and v_{max} values as found in the corresponding graph of the stationary state rates in Fig. 3. A similar plot for k_{out} and $[Ca]_i$ failed to linearize the data. Here again the results of the stationary state experiments suggested that the fraction of $[Ca]_i$ participating in the exchange rather than the overall cellular concentration would be the correct variable to insert. However, because of considerable scatter in the intracellular specific activities extrapolated to $t \to \infty$ at similar total Ca concentrations, the attempt to correct the data for unexchangeable Ca did not give meaningful results.

Sr- or ^{40}Ca-Activated ^{45}Ca "Countertransport"

If two substrates share a common saturable transfer system in the membrane and if a concentration gradient is established for one substrate (driving substrate) while the other substrate (driven substrate) is in equilibrium on the two sides of the membrane, the "downhill" movement of the driving substrate can induce countertransport, i.e., an uphill movement of the driven substrate in the opposite direction (Wilbrandt & Rosenberg, 1961). The demonstration of countertransport would provide further

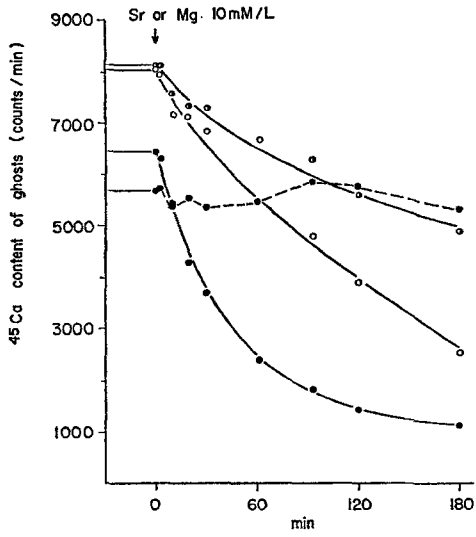

Fig. 7. Ca efflux from starved red cell ghosts as induced by the addition of Sr to the external medium ("counterflow"). Preparation of ghosts as in Fig. 1(*a*). The hemolyzing medium contained 0.25 (●——●, ● – – – ●), 0.5 (○——○), or 1 mM (◑——◑) of nonradioactive Ca and a constant amount of ^{45}Ca (~0.5 μC/ml). After 90 min of equilibration, enough Sr or Mg were added to increase the external concentration of these ions by 10 mM (arrow). The change in ^{45}Ca content of the ghosts suspended in 1 ml of the incubation medium (ordinate) in response to Sr (●——●, ○——○, ◑——◑) or Mg (● – – – ●) is plotted versus time. Note, that the specific activity of Ca on both sides of the membrane is identical. One of 4 similar experiments. Hematocrit: ~3%

evidence for a carrier-mediated Ca transport system in the membrane of metabolically depleted human red cell ghosts. To test this possibility, two series of experiments were performed in which Sr and ^{45}Ca or ^{40}Ca and ^{45}Ca were used as the two competing substrates. Sr was shown previously to possess some affinity for the red cell Ca transport system (Porzig, 1970).

A representative experiment is shown in Fig. 7. Erythrocyte ghosts loaded with different Ca concentrations were incubated under stationary state conditions. The specific activity of Ca was the same on both sides of the membrane. The experiment was started by adding enough Sr to achieve a concentration of 10 mM in the outside medium. The change in intracellular radioactivity following the addition of Sr is plotted versus time. Sr induced a considerable Ca outward movement which was uphill since $[Ca]_i$ was reduced well below $[Ca]_o$. The control experiment, in which Mg instead of Sr was used showed that the osmotic and concentration changes caused by the addition of 10 mM/liter incubation medium of a divalent

cation contained in a small volume (1 % or less of total extracellular volume) did not cause any measurable Ca efflux. Sr-induced Ca "countertransport" was peculiar in that the system did not return to the original equilibrium but reached a new equilibrium with a persistent inwardly directed Ca concentration gradient. A study of Sr net uptake under the conditions of the above experiments showed that the system did not equilibrate with respect to Sr; i.e., an inward Sr concentration gradient was maintained throughout the course of the experiment. In ghosts loaded with 0.5 mM Ca and incubated in the presence of up to 20 mM Sr, the ratio $[Sr]_o/[Sr]_i$ was still about 10 at the end of a 3-hr experiment.

Possibly Sr-activated Ca outflow in the "stationary state" was just sufficient to maintain the inward Ca concentration gradient. Because of the decreases in Sr uptake with time, the return to the original equilibrium might be too slow to be measurable during the experiment. Alternatively, the initial increase in cellular Sr might have decreased the Ca and Sr permeability of the membrane to such an extent that the inward Ca concentration gradient could be maintained even when the inward Sr movement ceased completely and no longer acted as a driving force for Ca outflow. The present experiments do not distinguish between these two possibilities. A counterflow phenomenon similar to Ca–Sr exchange was observed when ^{40}Ca–^{45}Ca was used instead as the competing pair of substrates. A constant amount of nonradioactive Ca was added to a ghost suspension previously equilibrated with respect to cellular and extracellular Ca concentrations. At the start of the experiment internal and external specific activities were identical. The sudden drop in specific activity on the outside induced an outward movement of tracer Ca which built up a concentration gradient for ^{45}Ca in the opposite direction. Fig. 8 relates the rate constants of Sr- or Ca-induced tracer efflux to the stationary state Ca concentration in the beginning of the experiment. The smaller the ratio of driving substrate to driven substrate, the slower was the efflux rate of the driven substrate. The actual numerical value of this ratio is determined by the relative affinities of the two substances for the membrane transport sites. Since 10 mM Sr (open symbols) and 1 mM Ca (closed symbols) were about equally effective, one can assume the relative affinities of Sr and Ca to be as 1:10.

Coupling between Ca and Sr Net Movements

In a previous study it was shown that in contrast to the tracer fluxes considered in the preceding paragraphs. Ca inward or outward net movements were not characterized by saturation kinetics (Porzig, 1972). In the

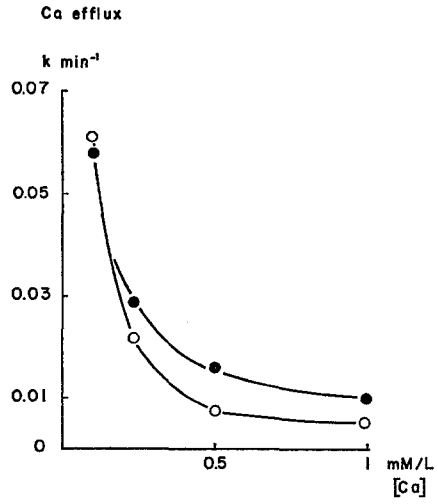

Fig. 8. Dependence of the rate constants of Sr- or ^{40}Ca-induced ^{45}Ca counterflow from red cell ghosts (ordinate, k min^{-1}) on the Ca concentration in the hemolyzing fluid (abscissa, mM/liter). Experimental procedure as described in Fig. 7. At the end of the equilibration period either 10 mM/liter $SrCl_2$ (○——○) or 1 mM/liter $CaCl_2$ (●——●) was added to the external medium. Evaluation of the rate constants as in Fig. 1 (*b*). The points are mean values from 4 experiments using Sr and 5 experiments using ^{40}Ca to induce ^{45}Ca countertransport

range of concentrations tested, Ca inflow and outflow appeared to be linearly related to $[Ca]_o$ or $[Ca]_i$, respectively. These previous results support the view that only the loaded form of the hypothetical carrier can move across the membrane and hence, the carrier is only capable of mediating exchange fluxes. To further substantiate this assumption. Sr-activated Ca net outflow was examined and compared to the movement of Ca in the absence of Sr. In the first set of experiments, Sr-activated Ca uphill transport and the concomitant Sr uptake were measured as a function of the external Sr concentration ($[Sr]_o$) (Fig. 9). The ghost cell suspensions were first equilibrated with respect to Ca so that no outwardly directed concentration gradient for this ion existed in the beginning of the experiment. Sufficient Sr was then added to establish a range of extracellular Sr concentrations between 1 and 20 mM. The results plotted in Fig. 9 confirmed the observations concerning Ca–Sr exchange reported above. Sr induced a net outward movement of Ca and, consequently, the formation of an inwardly directed Ca concentration gradient. In the presence of 15 to 20 mM Sr in the outside medium the ratio $[Ca]_o/[Ca]_i$ was changed from approximately 1:1 to approximately 2.5:1 (dashed curve in Fig. 9). In these experiments no fixed

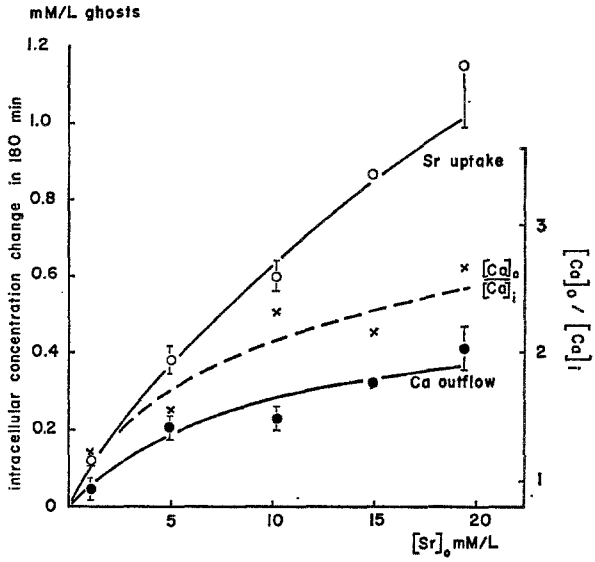

Fig. 9. Dependence of Sr-induced Ca net outflow, Sr net uptake and $[Ca]_o/[Ca]_i$ on $[Sr]_o$. Preparation of ghosts as in Fig. 1 (*a*). The hemolyzing medium contained 0.5 mM Ca. At the end of the equilibration period enough Sr was added to establish a range of external Sr concentrations between 1 and 20 mM. The net increase in $[Sr]_i$ (○——○) and the net decrease in $[Ca]_i$ (●——●) (left ordinate, mM/liter ghosts) was measured at the end of an incubation period of 180 min at 37 °C and plotted versus $[Sr]_o$ (abscissa, mM/liter). The dashed curve (× — — — ×, right ordinate) shows the ratio $[Ca]_o/[Ca]_i$ at the end of the incubation period for any particular $[Sr]_o$. The points on Sr uptake and Ca outflow curves are the mean of four measurements except for the values at 15 mM $[Sr]_o$ which are the mean of two measurements. Vertical bars indicate ± SE. The values for $[Ca]_o/[Ca]_i$ were taken from those three of these experiments in which the final $[Ca]_o$ had been measured. Hematocrit: 3.7 to 7.5 %

coupling seemed to exist between Sr inflow and Ca outflow. The ratio of Sr uptake to Ca outflow increased from 1.5 to 4 as $[Sr]_o$ was raised from 2 to 20 mM. Moreover, Sr-activated Ca outflow leveled off when $[Sr]_o$ was above 15 mM although Sr uptake in this concentration range was still far from saturation. If Sr and Ca indeed share a common transfer system, a stoichiometric coupling of the fluxes should exist. Since Sr and Ca ions both carry two charges the simplest assumption would be a one-for-one exchange. The most probable reason explaining the failure of the above experiments to demonstrate fixed coupling was that a considerable fraction of total Sr uptake did not take part in countertransport but probably represented "leak" flow and membrane-bound Sr (*see* p. 40).

In an attempt to separate Sr inflow coupled to Ca outflow from Sr uptake caused by other mechanisms (in the following paragraphs referred

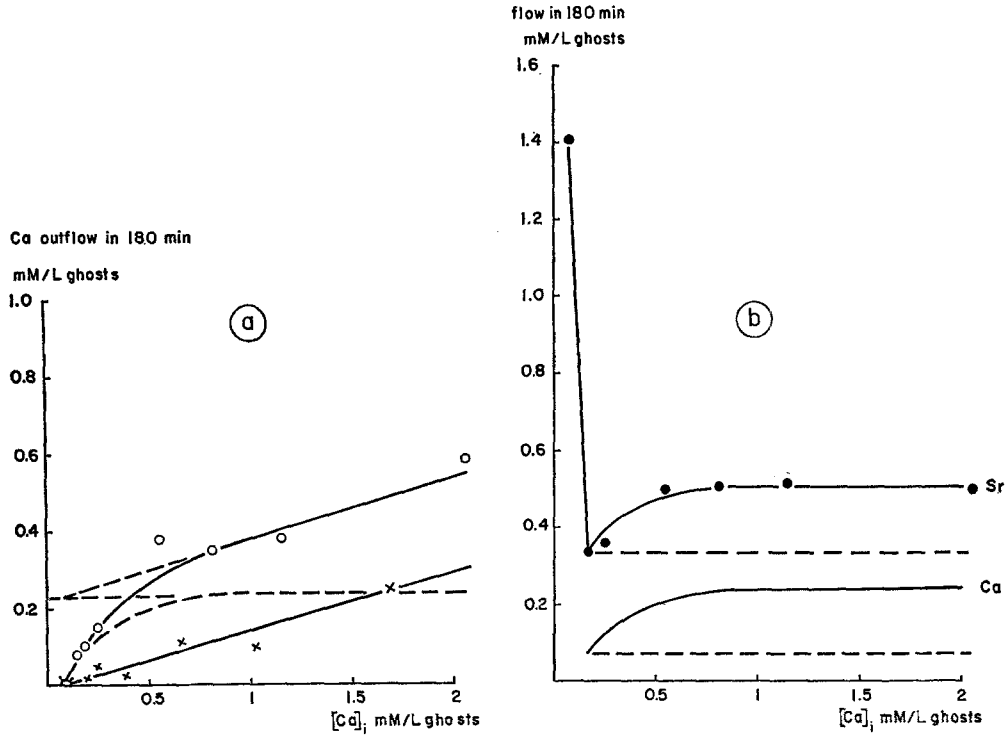

Fig. 10. Dependence of Sr-activated and Sr-independent Ca outflow and Ca-activated Sr inflow on $[Ca]_i$. Ghost preparation as described in Fig. 5. After the equilibration period, the ghosts were washed three times in Ca-free medium (140 mM KCl, 20 mM Tris–Cl, pH 7.4), then transferred to the incubation medium (37 °C) which either had the composition of the washing medium or differed from this solution in that 10 mM $SrCl_2$ replaced an equivalent amount of KCl and Tris–Cl (129 mM KCl, 18.5 mM Tris–Cl 10 mM $SrCl_2$, pH 7.4). Note, that the actual concentration of Sr in the suspension medium was only about 9 mM because of the inevitable dilution of the final suspension medium by washing medium carried over with the cell sediment. Hematocrit: 7.3 to 8.9%. One of 4 similar experiments. (*a*) The loss of cellular Ca in 180 min into a Sr-containing (o——o) or Sr-free (× – – ×) medium is plotted against the initial cellular Ca concentration. The dashed lines demonstrate the separation of a linear and a saturating component of Ca outflow into a Sr-containing medium. The saturating component is obtained by subtracting graphically Ca outflow in the Sr-free medium from Ca outflow in the Sr-containing medium. The saturating component represents Sr-activated Ca outflow. (*b*) Sr inflow in 180 min is plotted versus the initial cellular Ca concentration (• —— •). The $[Ca]_i$-dependent component of Sr inflow in the concentration range between 0.15 and 2.0 mM is marked by the dashed line parallel to the abscissa. To show that Ca-activated Sr inflow and Sr-activated Ca outflow are of similar magnitude, the corresponding part of the dashed curve in Fig. 10 (*a*) representing Sr-activated Ca outflow is replotted in Fig. 10 (*b*) (lower curve without experimental points). When $[Ca]_i$ was less than 0.15 mM Ca-activated Sr uptake was not separable from nonspecific Sr uptake

to as "unspecific" uptake), the dependence of Sr uptake and Ca–Sr exchange on $[Ca]_i$ was tested in the absence of external Ca. Ca-coupled Sr uptake should increase with increasing $[Ca]_i$ whereas unspecific Sr uptake should decrease as does Ca net uptake under similar conditions (Porzig, 1972). This effect would allow the analysis of exchange fluxes without interference from large unspecific Sr movements. Fig. 10 (*a*) shows Ca loss (open symbols) and Fig. 10 (*b*) Sr uptake (closed symbols) at constant $[Sr]_o$ and cellular Ca concentrations from 0.05 to 2.1 mM. The total change in cellular Sr and Ca at the end of an incubation period of 180 min at 37 °C is plotted versus the initial $[Ca]_i$. Initially, Ca was only present inside and Sr only outside of the cells. Therefore, both ions moved down their concentration gradients. Erythrocyte ghosts prepared in a Ca-free hemolyzing solution and suspended in isotonic buffered KCl-solution containing 9 mM Sr took up 1.4 mM Sr/liter cells (Fig. 10(*b*)). The incorporation of a small amount of Ca (0.15 mM) into ghost cells caused a reduction in Sr uptake of about 75%. Sr uptake increased again to 0.6 mM when $[Ca]_i$ was raised stepwise from 0.15 to 1 mM. Beyond 1 mM $[Ca]_i$ no further increase in Sr uptake was observed. These results suggested a saturable Ca-dependent component of Sr uptake which was superimposed on a large but rather constant nonspecific Sr gain.

In these and all following experiments, Ca and Sr net movements occurring during the time interval of 2 to 3 min between start of the experiment (suspension of the cells in the experimental medium) and withdrawal of the first sample were disregarded. Thus, rapid reactions such as displacement of extracellular Ca by Sr should not interfere with the experimental observations.

Ca outflow in the presence of 9 mM $[Sr]_o$ (open symbols in Fig. 10*a*) was not linearly related to $[Ca]_i$. The graphical analysis demonstrated in Fig. 10(*a*) suggested that this curve was again the sum of two components, one of which was linear and one of which became saturated with increasing $[Ca]_i$. The linear component was similar in magnitude to Ca outflow in the absence of external Sr measured in the same experiment and was therefore identified as the Sr-independent ("nonspecific") Ca loss (cross-symbols in Fig. 10*a*). The saturable component corresponded quantitatively to the Sr-activated fraction of Ca outflow obtained by subtracting the nonspecific fraction of Ca loss from total Ca outflow. Hence, specific and nonspecific movements of Ca from the cells into a Sr-containing medium seemed to be completely additive. Even though the slope of the straight line relating $[Ca]_i$ and nonspecific Ca outflow varied in four similar experiments, it was always close to the slope of the linear component of total Ca loss in the presence of Sr.

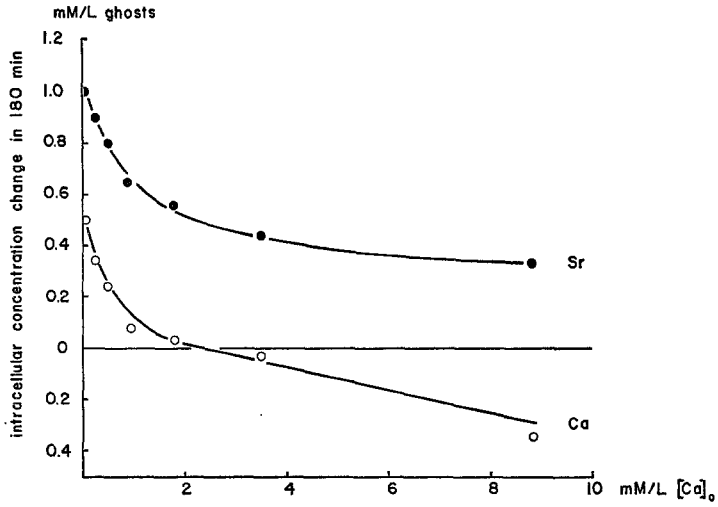

Fig. 11. Influence of $[Ca]_o$ on transmembrane Sr and Ca movements in starved red cell ghosts at constant $[Ca]_i$ and $[Sr]_o$. Preparation of ghosts as described in Fig. 5. The cellular Ca content at the beginning of the experiment was 0.75 mM (mean). The incubation medium contained 129 mM KCl, 10 mM $SrCl_2$, 18.5 mM Tris-Cl (pH 7.4). Different amounts of isotonic Ca solution were added to establish a range of external Ca concentrations between 0 and 10 mM. The cellular uptake or loss of Ca or Sr in 180 min is plotted versus $[Ca]_o$ (mean value of the Ca concentrations in the supernatant at the beginning and at the end of the experiment). The upper curve (● —— ●) shows the decrease in Sr uptake with increasing $[Ca]_o$ (i.e., with decreasing ratio $[Sr]_o/[Ca]_o$). The lower curve (○ ——○) depicts the decrease in Ca outflow under the same conditions. If $[Ca]_o$ was higher than 2.2 mM, net Ca uptake occurred (part of the curve below the parallel to the abscissa marking zero concentration change). One of 3 similar experiments. Hematocrit: 7.1 to 7.7%

In Fig. 10 (*b*), Sr-dependent Ca outflow is compared to Ca-dependent Sr uptake. Because of the large amount of nonspecific Sr uptake at a $[Ca]_i$ of less than 0.15 mM, this comparison was limited to a range of internal Ca concentrations between 0.16 and 2.1 mM. The lower curve in Fig. 10 (*b*) is identical with the dotted curve in Fig. 10 (*a*) and represents Sr-activated Ca outflow. The dashed line parallel to the abscissa was included to show which parts of the curves were actually compared. The Sr-activated Ca loss at any particular $[Ca]_i$ was identical in magnitude to the amount of Ca-activated Sr uptake.

These findings suggest that Ca and Sr can cross the membrane in a one-for-one exchange mediated by a specific transport system. Except for values of $[Ca]_i$ between 0.05 and 0.15 mM, the amount of unspecific Sr uptake (approximately 0.35 mM in 180 min at $[Sr]_o$ of 8.5 mM) in the concentration range between 0.2 and 2.5 mM appeared to be independent of $[Ca]_i$.

Mg outflow into a Sr-containing medium measured simultaneously in most of these experiments, was somewhat less than Mg loss into a Ca- and Sr-free medium. Hence, Mg did not seem to have any affinity to the Ca–Sr exchange system. On the other hand, the experiments indicate that external Sr did not increase the passive permeability of the ghosts.

To test whether the 1:1 Sr–Ca exchange ratio could also be demonstrated under the conditions of Sr-induced Ca uphill movement, Sr inward and Ca outward movements were studied as functions of $[Ca]_o$. As in the experiments described above, $[Sr]_o$ was 8.5 to 9 mM. The results of a representative experiment are shown in Fig. 11. Ca outflow and Sr uptake measured after 180 min of incubation at 37 °C decreased with increasing $[Ca]_o$. When $[Ca]_o$ was approximately 2.5 mM Ca outflow ceased completely and a further increase in $[Ca]_o$ led to a net Ca uptake. When Ca outward movement ceased, Sr uptake was not abolished but still amounted to 0.5 mM. With $[Ca]_o$ ranging between 2.5 and 10 mM, the cells gained Ca but the nonspecific Sr uptake was only slightly reduced and asymptotically approached a value of about 0.35 mM. If the amount of Sr uptake in the absence of any cellular net Ca concentration change (i.e., at 2.5 mM $[Ca]_o$) was subtracted from the total Sr uptake, the curves for Ca outward and Sr inward movements in Fig. 11 tended to coincide. This finding strongly supported the conclusion of a 1:1 exchange ratio for Sr-activated Ca efflux. Moreover, on the basis of the initial cellular Ca concentrations (mean: 0.714 mM), one can calculate that Ca outward movement ceased when the ratio $[Ca]_o/[Ca]_i$ was higher than 3. This figure is in reasonable agreement with the value of 2.5 as the highest concentration ratio achieved by Ca–Sr exchange in stationary state experiments (*see* Fig. 9).

Nonspecific Sr Uptake

In the preceding paragraphs the term "nonspecific Sr uptake" was defined as the increase in cellular Sr not caused by Ca–Sr exchange. The results suggest that two components of nonspecific uptake were present. As can be inferred from Figs. 10 (*b*) and 11, one of these components seemed to be largely independent of $[Ca]_o$ and $[Ca]_i$. In the experiment shown in Fig. 10 (*b*), the dashed line parallel to the abscissa marks this basic Sr uptake and separates it from Ca-dependent uptake. In the experiment illustrated in Fig. 11, $[Sr]_o$ was the same as in the experiment shown in Fig. 10 (*b*) and a similar value of nonspecific Sr uptake was approached asymptotically when $[Ca]_o$ was increased to 9 mM. The small influence of $[Ca]_o$ strongly suggests that this fraction of Sr uptake represents a "leak" flux into the

cell down the Sr concentration gradient rather than binding of Sr to membrane sites. On the other hand, the considerable increase in Sr uptake which was observed when ghosts were prepared in the absence of Ca (*see* Fig. 10*b*) may be caused mainly by Sr binding to membrane sites. This assumption is supported by earlier observations showing that the ghost membrane under these conditions has a particularly large Ca binding capacity (Porzig, 1972).

Discussion

In two earlier studies on ^{45}Ca efflux and on Ca net movements in human red cell ghosts (Porzig, 1970, 1972) tracer efflux on the basis of saturability and ion specificity was interpreted in terms of a carrier-mediated exchange diffusion. However, net movements driven by inward or outward concentration gradients did not obey carrier kinetics. The present work confirms and extends these findings. It provides evidence that the ATP-independent Ca transfer system is limited to the mediation of a tightly coupled one-for-one exchange diffusion across the membrane with Ca or Sr being accepted as the transported substrates. The conclusions are based on the following experimental findings. (1) The transfer system was characterized by similar kinetics for efflux and influx (Figs. 2, 4, 5 and 6). (2) Tracer flux rate constants were nearly the same in stationary and nonstationary state experiments (Figs. 2, 5 and 6). Even in the presence of outward Ca concentration gradients of up to 2 mM or inward gradients of up to 8 mM, these rate constants did not change in the course of an experiment. (3) Countertransport of ^{40}Ca and ^{45}Ca induced by extracellular Sr or of ^{45}Ca induced by extracellular ^{40}Ca resulted in persisting deviations from stationary state concentrations. An inwardly directed concentration gradient of the driven substrate was established and maintained during the course of the experiment. The driving substrate did not equilibrate (Fig. 7). One-for-one coupled Sr–Ca exchange in net flow experiments was additive to downhill net Ca and Sr movements (Fig. 10 *a*, *b*).

A comparison of influx and efflux rate constants as functions of $[Ca]_o$ and $[Ca]_i$ to test the concept of a symmetric membrane Ca transport system is valid only if the kinetic compartments are the same for influx and efflux. Ca net flow studies have shown previously (Porzig, 1972) that this assumption is not justified if Ca-containing and Ca-free ghosts are to be compared. In the latter but not in the former case, the membrane constitutes a large additional compartment for Ca uptake. Therefore, ghosts included in ^{45}Ca flux studies contained not less than 0.1 mM Ca. The upper limit was set at 3 mM to avoid the pronounced leakage of Ca out of the cells known to occur at $[Ca]_i$ above 4 mM. Under these conditions, Ca fluxes in both

directions should follow two-compartment kinetics. Even though linear semilog plots of cellular tracer content versus time show that first-order kinetics are a good approximation for efflux, no similar direct test was possible for influx. However, in stationary state experiments, the values for inward rate constants calculated on the assumption of a first-order process for influx agreed so well with the values for k_{in} derived from initial velocities that there is no reason to suspect different kinetics for efflux and influx.

Even when single rate constants for ^{45}Ca influx and efflux are taken for granted, one is still left with the problem of whether the small differences in the numerical values for k_{in} and k_{out} reported above (Figs. 2, 4, 5 and 6) indicate a true asymmetry of the exchange system. The internal Ca concentration on which the comparison of flux rates must be based is unknown. The exchangeable fraction of cellular Ca used in the present experiments was only the upper limit of the "effective" concentration actually "seen" by the transport site on the inner surface of the membrane. Indeed, earlier experiments designed to evaluate the internal free Ca concentration ($[Ca^{++}]_i$) as a function of total cellular concentration suggested a considerable fraction of Ca to be bound to membrane sites (Porzig, 1972). The exchangeable fraction in the present investigation was larger than $[Ca^{++}]_i$ determined at comparable cellular Ca concentrations in this previous study. Such discrepancies between exchangeable and free Ca would explain the finding that k_{in} at any particular Ca concentration seemed to be smaller than k_{out} even if total cellular Ca was corrected for exchangeable Ca. Consequently, it would also explain the difference in Km values for efflux and influx (Fig. 4).

The argument that $[Ca^{++}]_i$ is only part of the total amount of exchangeable Ca implies that inexchangeable and exchangeable fractions of cellular Ca define kinetic or functional compartments rather than morphological (e.g., membrane and intracellular space) ones. It is possible that Ca_{inex} represents a tightly bound fraction of membrane Ca which exchanges very slowly with external Ca. However, the fact that nonexchangeable Ca is almost completely released by rehemolysis of the ghost in a hypotonic medium rather suggests a kinetic inhomogeneity of the ghost population. The latter hypothesis accounts for Ca_{inex} by assuming a fraction of the ghost to be nearly impermeable to Ca and thus not to take part in the exchange. The size of this fraction is assumed to vary with $[Ca]_i$ (Porzig, 1970).

In previous studies on Ca exchange diffusion in biological membranes, particularly in smooth and striated muscle it was difficult to estimate the contribution of membrane-bound Ca to total cellular Ca exchange (Shanes & Bianchi, 1959; van Breemen, Daniel & van Breemen, 1966; Feinstein, 1966; van Breemen & van Breemen, 1968). The available evidence suggests

that the number of membrane binding sites accessible for extracellular Ca was rather limited in red cell ghosts prepared in the presence of no less than 0.1 mM Ca (Porzig, 1972). Probably the amount of Ca bound to these sites was only a small fraction of total cellular Ca and contributed little to the exchange movements measured in the present study. Additional support for this assumption comes from the following observations. (1) Under comparable conditions, the rate of ^{45}Ca efflux was similar in magnitude irrespective of whether it was calculated from influx experiments (this paper) or efflux experiments (Porzig, 1970). (2) In the range of concentrations tested, 50 to 90% of total cellular Ca was exchangeable within 180 min. The exchange followed the kinetics of a simple two-compartment system. (3) The rate of Ca uptake into Ca-loaded ghosts was much slower than the rate of Ca binding to fragmented red cell membranes. In the latter preparation uptake was complete in less than 10 min (Gent, Trounce & Walser, 1964).

An important aspect of the present study is the demonstration that saturable Ca–Sr countertransport in net flow experiments is additive to nonsaturating downhill net Ca or Sr movements. Except for ghosts prepared in Ca-free medium which exhibit a large nonspecific Sr binding capacity (Fig. 10), a one-for-one Ca-Sr coupling was maintained over the entire experimental range of intracellular Ca concentrations. These observations strongly suggest separate pathways for net and exchange movements. A transport system restricted to transmembrane specific exchange and incapable of mediating net movements similar to those described in this study for Ca and Sr, fits both into the concepts of Ussing (1947; 1960) for exchange diffusion and Stein (1967) for compulsory exchange diffusion. It can be interpreted in terms of a carrier-mediated transfer mechanism where the loaded but not the free carrier can move across the membrane.

Thus, a Ca transport system limited to exchange diffusion processes will not contribute to build up an asymmetric ion distribution between cells and medium. Hence, nonequilibration observed with respect to net Ca and Sr inward movements must be attributed to other mechanisms regulating membrane permeability for these ions. Previous experiments suggested that membrane-bound Ca restricts Ca uptake in erythrocyte ghosts (Porzig, 1972). The present experiments showed that transmembrane exchange occurred in spite of an almost complete inhibition of net inward movements. These results do not necessarily require the assumption of separate pathways for exchange and net transfer of Ca across the membrane. It is conceivable that Ca bound to specific sites at the inner face of the membrane restricts the mobility of the unloaded carrier. In this case with increasing $[Ca]_i$, Ca membrane transfer will be more and more limited to exchange movements.

However, the finding that Sr activated Ca outflow is additive to net Ca movements over a large range of internal Ca concentrations rather supports the two-pathway hypothesis.

It is most tempting to assume that the exchange movement occurs by means of the same system which is known to mediate active Ca outward transport in red cells (Lee & Shin, 1969; Schatzmann & Vincenzi, 1969). Other ion transport systems were shown to possess the capacity of catalyzing ion exchange instead of pumping. In red cells and squid axon the Na–K pump under certain conditions effects a Na–Na exchange (Garahan & Glynn, 1967*a*, *b*; Baker, Blaustein, Keynes, Manil, Shaw & Steinhardt, 1969). Similarly in sarcoplasmic reticulum vesicles, the Ca pump is also able to bring about Ca–Ca or Ca–Sr exchange (Weber, Herz & Reiss, 1966; Weber, 1971). Even though a one-for-one exchange of ions does not necessarily involve the consumption of energy, these pump-mediated exchange reactions only occur in the presence of nucleotide triphosphates (*cf.* Weber *et al.*, 1966; Glynn, Hoffman & Lew, 1971).

In red cell ghosts, no comparable intimate relationship exists between active Ca or Sr net transport and the exchange of these ions across the membrane. Exchange movements proved to be ATP-independent and to occur in metabolically depleted cells. From the data of Weed, LaCelle and Merill (1969) it was estimated that not more than 10 μM/liter of cells of ATP were left in the ghost preparation used in this study. Furthermore, Ca and Sr had similar affinities for the sites affecting active net outward movements (Olson & Cazort, 1969; Schatzmann & Vincenzi, 1969), while in the present exchange experiments, Sr had a lower affinity towards transport sites than did Ca. Olson and Cazort (1969) did not take into account such differences in affinities and therefore failed to recognize a Sr-induced Ca transport in the absence of ATP. However, their experiments indicate that Ca–Sr exchange is not enhanced in the presence of ATP. It is therefore possible that Ca exchange in red cells is not mediated by the Ca pump but rather uses a pathway which is related to the Ca exchange mechanisms widespread in tissues lacking a Ca pump of the red cell type. Such transport systems were described in squid axon (Baker, Blaustein, Keynes, Manil, Shaw & Steinhardt, 1969), mammalian cardiac muscle (Reuter & Seitz, 1968; Glitsch, 1969; Glitsch, Reuter & Scholz, 1970), skeletal muscle (Shanes & Bianchi, 1959), uterine smooth muscle (van Breemen *et al.*, 1966; Feinstein, 1966; Krejci & Daniel, 1970) and vascular smooth muscle (Reuter, Blaustein & Häusler, 1972). As in red cells, these transport systems accept Sr but not Mg to replace Ca. They differ from a red cell Ca transfer system in that most of them also exchange Na for Ca and thus utilize the

inwardly directed sodium concentration gradient to expel Ca against its own concentration gradient from the cell interior. These systems are also dependent on the trans-concentrations of the ions involved and indicate unequal mobility of loaded and unloaded carrier (*cf.* Glitsch *et al.*, 1970). Red cells cannot use hetero-exchange diffusion to achieve an uphill net Ca outward movement because the physiological exchange candidates, particularly Na and Mg have no affinity for the Ca transfer system (Porzig, 1970). Nevertheless, the red cell Ca transport system provides a useful biological model to study the mechanisms which enable cells to build up transmembrane ion concentration gradients without the expenditure of metabolic energy.

The above-mentioned exchange mechanisms were interpreted as reflecting carrier-mediated ion transfer. An alternative possibility is suggested by the work of van Breemen & van Breemen (1969) on ion exchange across an artificial porous phospholipid membrane. According to these authors, interdiffusion of ions across charged pores of an ion exchange membrane may result in kinetics similar to carrier-mediated exchange diffusion.

I am indebted to Profs. H. Reuter and J. Bassingthwaighte and Dr. M. Touabi for helpful discussions and critical suggestions during the course of this study. The technical assistance of Miss M. Over, Mr. M. Staub and Mr. R. Binggeli is greatfully acknowledged.

This study was supported by the Swiss National Science foundation Grant No.3.61.69 to Prof. H. Reuter.

References

Baker, P. F., Blaustein, M. P., Hodgkin, A. L., Steinhardt, R. A. 1969. The influence of calcium on sodium efflux in squid axons. *J. Physiol.* **200**:431.

Baker, P. F., Blaustein, M. P., Keynes, R. D., Manil, J., Shaw, T. I., Steinhardt, R. A. 1969. The oubain-sensitive fluxes of sodium and potassium in squid giant axons. *J. Physiol.* **200**:459.

Blaustein, M. P., Hodgkin, A. L. 1969. The effect of cyanide on the efflux of calcium from squid axons. *J. Physiol.* **200**:497.

Breemen, C. van, Breemen, D. van. 1968. Stimulation of ^{45}Ca efflux from smooth muscle by extracellular Ca^{2+}. *Biochim. Biophys. Acta* **163**:114.

Breemen, D. van, Breemen, C. van. 1969. Calcium exchange diffusion in a porous phospholipid ion-exchange membrane. *Nature* **223**:898.

Breemen, C. van, Daniel, E. E., Breemen, D. van. 1966. Ca distribution and exchange in the rat uterus. *J. Gen. Physiol.* **49**:1265.

Ekman, A., Manninen, V., Salminen, S. 1969. Ion movements in red cells treated with propranolol. *Acta Physiol. Scand.* **75**:333.

Feinstein, M. B. 1966. Inhibition of contraction and calcium exchangeability in rat uterus by local anesthetics. *J. Pharmacol.* **152**:516.

Garrahan, P. J., Glynn, I. M. 1967*a*. The behaviour of the sodium pump in red cells in the absence of external potassium. *J. Physiol.* **192**:159.

Garrahan, P. J., Glynn, I. M. 1967*b*. Factors affecting the relative magnitudes of the sodium:potassium and sodium:sodium exchange catalyzed by the sodium pump. *J. Physiol.* **192**:189.

Gent, W. L. G., Trounce, J. R., Walser, M. 1964. The binding of calcium ion by the human erythrocyte membrane. *Arch. Biochim. Biophys.* **105**:582.

Glitsch, H. G. 1969. Über die Wirkung von Sr-Ionen auf den Ca^{2+}-Austausch am Meerschweinchenvorhof. *Experientia* **25**:612.

Glitsch, H. G., Reuter, H., Scholz, H. 1970. The effect of the internal sodium concentration on calcium fluxes in isolated guinea-pig auricles. *J. Physiol.* **209**:25.

Glynn, I. M., Hoffman, J. F., Lew, V. L. 1971. Some "partial reactions" of the sodium pump. *Phil. Trans.* **262**:91.

Kalix, P. 1971. Uptake and release of calcium in rabbit vagus nerve. *Pflüg. Arch. Ges. Physiol.* **326**:1.

Krejci, I., Daniel, E. E. 1970. Effect of altered external calcium concentration on fluxes of calcium 45 in rat myometrium. *Amer. J. Physiol.* **219**:263.

Lamb, J. F., Lindsay, K. 1971. Effect of Na, metabolic inhibitors and ATP on Ca movements in L cells. *J. Physiol.* **218**:691.

Lee, K. S., Shin, B. C. 1969. Studies on the active transport of calcium in human red cells. *J. Gen. Physiol.* **54**:713.

Manninen, V. 1970. Movements of sodium and potassium ions and their tracers in propranolol-treated red cells and diaphragm muscle. *Acta Physiol. Scand.* (Suppl.) **355**:1.

Olson, E. J., Cazort, R. J. 1969. Active calcium and strontium transport in human erythrocyte ghosts. *J. Gen. Physiol.* **53**:311.

Porzig, H. 1970. Calcium efflux from human erythrocyte ghosts. *J. Membrane Biol.* **2**:324.

Porzig, H. 1972. ATP-independent calcium net movements in human red cell ghosts. *J. Membrane Biol.* **8**:237.

Reuter, H., Blaustein, M. P., Häusler, G. 1972. Na–Ca exchange and tension development in arterial smooth muscle. *Phil. Trans.* (*In press*).

Reuter, H., Seitz, N. 1968. The dependence of calcium efflux from cardiac muscle on temperature and external ion composition. *J. Physiol.* **195**:451.

Riggs, D. S., 1963. The Mathematical Approach to Physiological Problems. p. 277. The William & Wilkins Company, Baltimore, Maryland.

Rossum, G. D. V. van. 1970. Net movements of calcium and magnesium in slices of rat liver. *J. Gen. Physiol.* **55**:18.

Schatzmann, H. J., Vincenzi, F. F. 1969. Calcium movements across the membrane of human red cells. *J. Physiol.* **201**:369.

Shanes, A. M., Bianchi, C. P. 1959. The distribution and kinetics of release of radiocalcium in tendon and skeletal muscle. *J. Gen. Physiol.* **42**:1123.

Stein, W. D. 1967. The Movements of Molecules across Cell Membranes. p. 156. Academic Press Inc., New York, London.

Ussing, H. H. 1947. Interpretation of the exchange of radiosodium in isolated muscle. *Nature* **160**:262.

Ussing, H. H. 1960. The alkali metal ions in isolated systems and tissues. *In*: Handbuch der Experimentellen Pharmakologie. Vol. 13, p. 50. Springer-Verlag, Berlin.

Weber, A. 1971. Regulatory mechanisms of the calcium transport system of fragmented rabbit sarcoplasmic reticulum. I. The effect of accumulated calcium on transport and adenosine triphosphate hydrolysis. *J. Gen. Physiol.* **57**:50.

Weber, A., Herz, R., Reiss, I. 1966. Study of the kinetics of calcium transport by isolated fragmented sarcoplasmic reticulum. *Biochem. Z.* **345**:329.

Weed, R. I., LaCelle, P. L., Merrill, E. W. 1969. Metabolic dependence of red cell deformability. *J. Clin. Invest.* **48**:795.

Wilbrandt, W., Rosenberg, T. 1961. The concept of carrier transport and its corollaries in pharmacology. *Pharmacol. Rev.* **13**:109.